Effects of Metallographic Structures on the Properties of High-Performance Phosphor Bronze

by Kuniteru Mihara *, Tatsuhiko Eguchi *, Takashi Yamamoto *2 and Akihiro Kanamori *2

ABSTRACT As electronic equipment such as mobile phones become more compact, higher in mounting density and lower in profile in recent years, connector materials for these equipment are required to be higher in strength and better in bending workability. In response to such requirements, Furukawa Electric has developed F5218 and F5248 alloys, new versions of phosphor bronze for springs with smaller grain size, achieving improved strength and bending workability [1]. In this work, the following conclusions were reached: the grain size and strength in recrystallized structures can be described by the Hall-Petch relationship; the strength and bending workability improve as grain size is reduced; irrespective of their small grain size, degradation in the stress relaxation is suppressed due to Fe-(Ni)-P precipitates; and their grain growth rates are lower than those of C5210 and C5240 due to the contribution of P precipitates that suppress the growth.

1. INTRODUCTION

As electronic equipment such as mobile phones become more compact, higher in mounting density and lower in profile in recent years, connector materials for these equipment are required to be higher in strength and better in bending workability.

Phosphor bronze has been widely used in connectors and relay contacts thanks to its low Young's modulus and high spring characteristics, i.e. strength. However, phosphor bronze generally degrades in bending workability when heavily worked for work hardening. To improve such characteristics, Furukawa Electric developed F5218 and F5248 alloys, new versions of phosphor bronze for springs with smaller grain size, provided with improved strength and bending workability.

In this work, we continued the study on reducing the grain size, and succeeded in combining high strength and superior bending workability. This report will describe the effects of small grain on the alloy properties as well as the structure control technology.

2. EXPERIMENTAL METHODOLOGY

Table 1 shows the compositions of F5218 and F5248 developed here, and those for C5210 and C5240 are included for comparison. As shown, the alloys developed here have a small addition of Fe and Ni to the base copper alloys containing respectively 8 % and 10 % of Sn. The items and methods of characteristics evaluation of these alloys will be described below.

* Metals Research Center, R&D Division
*2 Metals Co.

Table 1 Chemical compositions of the alloys. (mass%)

	Sn	P	Fe	Ni	Cu
F5218	8	0.04	0.1	0.05	Balance
F5248	10	0.04	0.1	0.05	Balance
C5210	8	0.15	—	—	Balance
C5240	10	0.15	—	—	Balance

2.1 Mechanical Characteristics

The tests were carried out using an Instron type testing machine and JIS No. 5 test specimens, under the conditions of gage length: 50 mm and cross head speed: 10 mm/min at room temperature to obtain tensile strength (TS), 0.2 % yield strength (YS) and elongation (El).

2.2 Measurement of Grain Size

Grain size was measured in cross sections perpendicular to the rolling direction in conformity with JIS H 0501, whereby the specimen was mechanically polished and surface etched, and photographs were taken using an optical microscope and a scanning electron microscope (SEM) to evaluate the grain size using the method of section. More than 100 crystal grains were measured and the averaged grain size was obtained.

2.3 Bending Workability

90-degree W-bend tests without lubrication were carried out using a 1-ton pressing machine. Specimens were cut perpendicular to the rolling direction to effect "bad-way bending," and the minimum bending radius R at which no cracking occurred was evaluated to calculate the minimum bending radius/thickness ratio expressed by R/t, an indicator of bending workability.

2.4 Stress Relaxation Test

The tests were carried out by the cantilever method in conformity with EMS-3003, the standard of the Electronic Materials Manufacturers Association of Japan. The loading stress was set to YS x 0.8, and heating was done at 150°C in ambient atmosphere using an air bath.

2.5 Transmission Electron Microscope (TEM) Observation

TEM specimens were prepared by the twin-jet polishing method, and observations were made using JEM-3010 equipped with an energy dispersive X-ray spectrometer (EDS) at an acceleration voltage of 300 kV.

3. EXPERIMENTAL RESULTS AND DISCUSSIONS

3.1 Grain Size and Hall-Petch Relationship

Figure 1 shows the grain size dependence of mechanical characteristics (TS and YS) of annealed F5218. The mechanical characteristics show a linear dependence on $d^{-1/2}$, where d represents the grain size, and it can be seen that the smaller the grain size, the higher the strength, i.e. the Hall-Petch relationship. Moreover, when the gradients of dependence are compared between TS and YS, YS is seen to be higher in the gradient indicating a higher susceptibility on grain size. Meanwhile, such a relationship was confirmed with F5248, C5210 and C5240. In this study, various characteristics will be compared among the three grain sizes of $d^{-1/2} \fallingdotseq 0.31$ ($d \fallingdotseq 10\ \mu$m), $d^{-1/2} \fallingdotseq 0.46$ ($d \fallingdotseq 4.7\ \mu$m) and $d^{-1/2} \fallingdotseq 0.75$ ($d \fallingdotseq 1.8\ \mu$m).

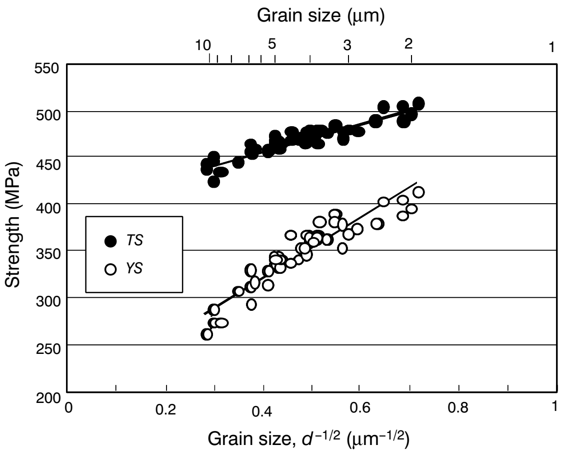

Figure 1 Grain size dependence of strength of F5218.

3.2 Relationship between Grain Size and Bending Workability

Figure 2 shows the evaluated results of the bending workability represented by R/t of F5218 and F5248 with three different grain sizes. In the Figure, the R/t of materials having YS of approximately about 650 MPa, 700 MPa and 750 MPa at each grain size were plotted at appropriate points, and then the points belonging to the same YS values were connected by a single line. It can be seen that the bending workability of an F5218 material with $YS \fallingdotseq 750$ MPa shown in Figure 2 (a), for example, exhibits improvements such that the R/t value decreases as the grain size becomes smaller over the course of $d^{-1/2} \fallingdotseq 0.31$, $d^{-1/2} \fallingdotseq 0.46$ and $d^{-1/2} \fallingdotseq 0.75$. This tendency can be identified in the other YS values and with F5248 alloy as shown in Figure 2 (b), indicating that reducing the grain size results in the improvement of bending workability.

That is to say, reducing the grain size can achieve combining high strength and good bending workability.

It is reported that improvements in bending workability by reducing the grain size result from a process such that the traveling distances of dislocations shorten when the material is subjected to bending, so that stress concentration due to the accumulation of dislocations is reduced thereby improving the fracture toughness [2]. An alternative explanation is that the grain boundary areas are enlarged due to the reduction of grain size, thus enhancing the effects to disperse the stress caused by bending.

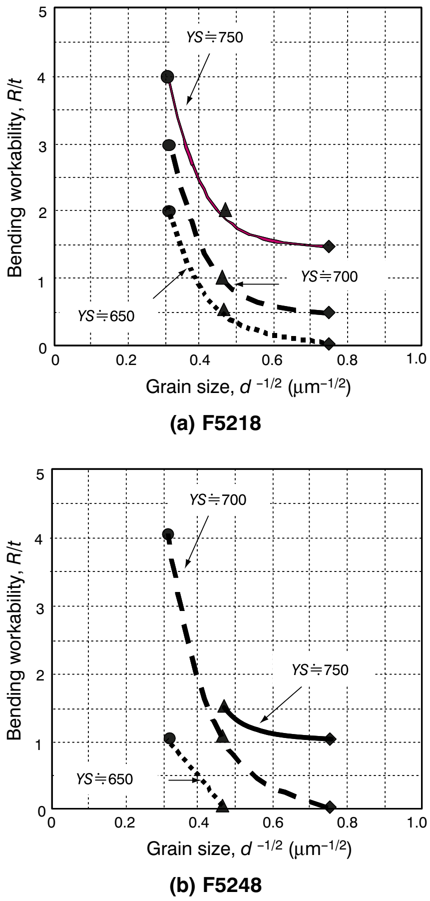

Figure 2 Relationship between bending workability and grain size of selected alloys.

3.3 Stress Relaxation Characteristics

Figures 3 (a) and 3 (b) show the relationship between the stress relaxation and the grain size represented by $d^{-1/2}$ of F5218 and C5210, and of F5248 and C5240, respectively. The stress relaxation characteristics of every alloy deteriorate as the grain size reduces. The explanation for this commonly known tendency is that the contribution of diffusive creep grows in the thermally activated state, and that the mean free path of moving dislocations shortens due to the large areas of boundaries [3].

However, when the stress relaxation characteristics of F5218 are compared with C5210, and F5248 with C5240, for the same grain size, it can be seen that F5218 and F5248 show better performance than their counterparts. When the grain size dependency of each alloy is approximated using a straight line, the gradients for F5218 and F5248 are less steep than those for C5210 and C5240, indicating lower susceptibilities to the changes in grain size.

The reason why F5218 and F5248 have superior stress relaxation characteristics may be explained by a hypothesis such that the small amount of Fe and Ni additives form Fe-(Ni)-P precipitates thus pinning down the moving dislocations in the thermally activated process [1].

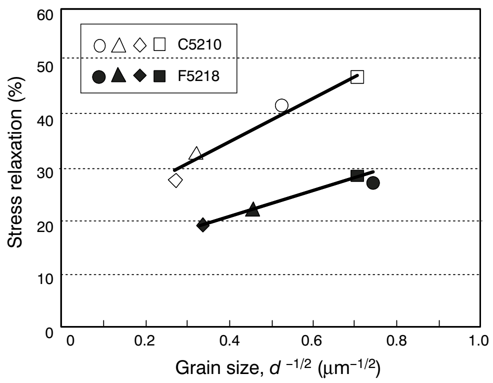

(a) F5218 and C5210

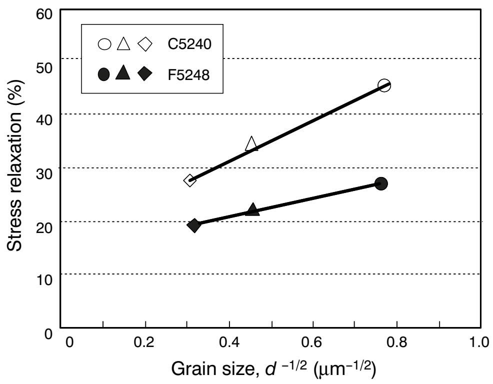

(b) F5248 and C5240

Figure 3 Stress relaxation characteristics of selected alloys.

3.4 Grain Growth and Fe-(Ni)-P Precipitates

As was described in Section 3.2, reducing grain size can realize good alloy performance combining strength and bending workability, but it is necessary to establish an industrial technique to obtain small grain size in a stable manner.

Specimens of F5218, F5248, C5210 and C5240 were heat treated under an equi-temporal heat treatment (batch-type heat treatment) of 300~500°C for 2 hr to investigate their recrystallization behavior. As a result, it was confirmed that the primary recrystallization temperatures for F5218 and F5248 and those for C5210 and C5240 were 360°C and 340°C, respectively. Figure 4 shows the results of investigation on the grain size after the specimens were heat treated at temperatures higher than the recrystallization temperatures. It can be seen from Figure 4 that there is much difference in the growth rate of grain size between F5218 and C5210, and between F5248 and C5240. Specifically, it was confirmed that C5210 grew in grain size at temperatures higher than the recrystallization temperature resulting in the increase in the grain size, whereas F5218 was suppressed in grain growth thus maintaining the small grain size even at a temperature higher than the recrystallization temperature by 50°C.

TEM observations were made to investigate the reason of suppression of grain growth in F5218 and F5248. Figure 5 (a) shows the structure of recrystallized F5218. From this TEM image, precipitates of 50 nm in size (indicated by the arrows) are formed on the recrystallization boundaries thereby suppressing the growth of grains. The precipitates were analyzed using the EDS equipped on the TEM, and it was confirmed that they are Fe-(Ni)-P precipitates as illustrated in Figure 5 (b).

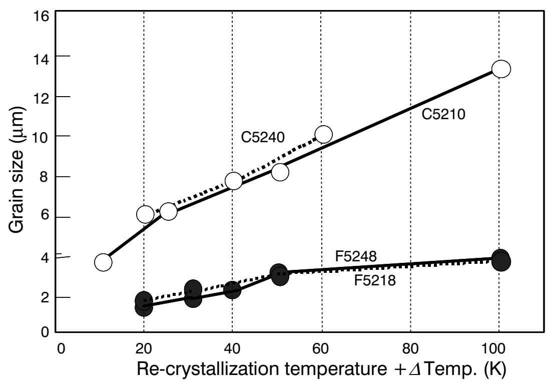

Figure 4 Relationship between grain size and heat treatment temperature.

3.5 Evaluation of Effects of Secondary Phase Using Classical Recrystallization Rate Equation

It has been shown that the Fe-(Ni)-P precipitates suppress grain growth achieving small grains in a stable manner. Then we proceeded to evaluate the effects of secondary phase using the classical recrystallization equation. The following calculating formulas were used [4].

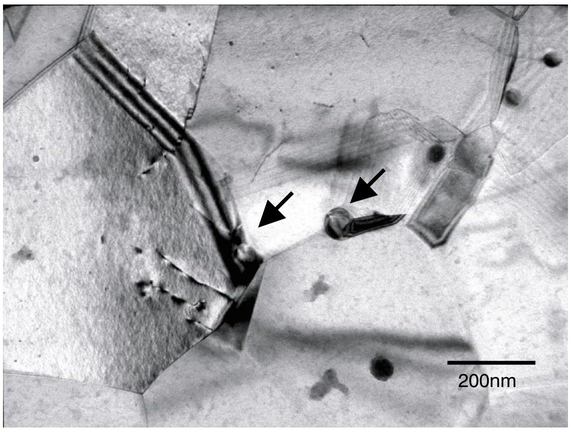

(a) Bright image with the arrows indicating precipitates

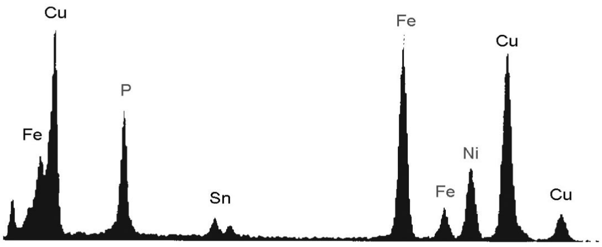

(b) EDS chart of precipitates

Figure 5 TEM image and EDS analysis of F5218.

1) Rate of change in recrystallized grain size R

$$dR/dt = MV(\Delta G + 3\gamma_1/R - 3f\gamma_2/2r) + J/N(Rc - R + \delta R/2) \quad (1)$$

where: ΔG is the driving force for recrystallization,

γ_1 and γ_2 are the interfacial energy for different phases of recrystallization, f is the volume fraction of precipitate, Rc is the critical nucleus size, δR is fluctuation of the critical nucleus size identical to 1.1 Rc, M is the mobility of grain boundary, V is mole volume, t is time, and r is the size of recrystallized grain.

2) Change in recrystallized grain density N

$$dN/dt = J \quad (2)$$

where: J is the generation rate of recrystallization nucleus in the classical theory.

3) Change in recrystallization ratio

$$d\ln(1 - X)/dt = -4/3\pi \cdot J \cdot R^3 \quad (3)$$

Figure 6 (a) and 6 (b) show the calculated results at 400°C (673 K) of grain growth and the recrystallization ratio over time of F5218 and C5210, respectively, where parameters γ_1= 0.6 J/m^2 and γ_2=0.85 J/m^2 were used [4]. Comparing the grain growth between C5210 and F5218 having the secondary phase, the latter is seen to be slow in the grain growth rate. Moreover, from Figure 6 (b) where the recrystallization ratio is shown, it is suggested that the recrystallization behavior is delayed in F5218 having the secondary phase.

It is thought that the reason the reduction in grain size is brought about under the existence of secondary phase is that: 1) after primary recrystallization is completed, the secondary phase pins down the grain boundaries to suppress grain growth; and 2) new recrystallization nuclei are generated in the regions where grain growth is suppressed. And it is estimated that by this mechanism F5218 and F5248 having secondary phase achieve grain size reduction rather easily.

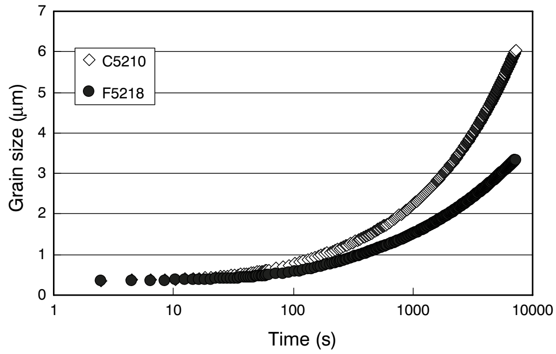

(a) Grain growth

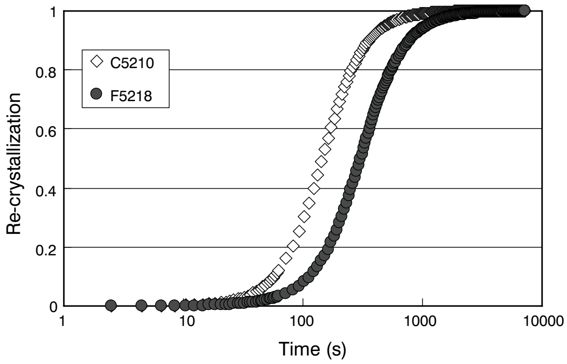

(b) Recrystallization ratio

Figure 6 Calculated grain growth and recrystallization ratio.

4. CONCLUSION

Effects of metallographic structures on the properties of F5218 and F5248, i.e. new phosphor bronze for springs with a small addition of Fe and Ni, were studied, and the following conclusions were reached.

1) The grain size and strength in recrystallized structures can be described by the Hall-Petch relationship, and by this correlation it is shown that the yield strength is more susceptible to grain size than the tensile strength is.
2) By reducing the grain size, F5218 and F5248 alloys with high strength and good bending workability have been developed.
3) Grain growth rate after primary recrystallization of F5218 and F5248 is lower than that of C5210 and C5240, and it is confirmed that phosphor precipitates contribute to suppressing and retarding the grain growth.

4) F5218 and F5248 with phosphor precipitates show little degradation in stress relaxation characteristics irrespective of reduced grain size, which is also shown to be attributable to contributions of phosphor precipitates.

REFERENCES

1) K. Mihara: Transactions of Japan Copper and Brass Association, 41, 210 (2002). (in Japanese)
2) Y. Murakami: Journal of The Japan Institute of Metals, 17, 190 (1978). (in Japanese)
3) J. Miyake: Transactions of Japan Copper and Brass Workshop, 32, 63 (1993). (in Japanese)
4) H. Fujiwara: Journal of The Japan Institute of Metals, 40, 14 (1999).